Magnetic Resonance Volume Flow and Jet Velocity Mapping in Aortic Coarctation

RAAD H. MOHIADDIN, MD, PHILIP J. KILNER, MB, SIMON REES, FRCR,
DONALD B. LONGMORE, FRCS

London, England, United Kingdom

Objectives. Nuclear magnetic resonance (MRI) velocity mapping was used to characterize flow waveforms and to measure volume flow in the ascending and descending thoracic aorta in patients with aortic coarctation and in healthy volunteers. We present the method and discuss the relation between these measurements and aortic narrowing assessed by MRI. Finally, we compare coarctation jet velocity measured by MRI velocity mapping with that obtained from continuous wave Doppler echocardiography.

Background. The development of a noninvasive imaging method for morphologic visualization of aortic coarctation and for measurement of its impact on blood flow is highly desirable in the preoperative and postoperative management of patients.

Methods. Magnetic resonance imaging phase-shift velocity mapping was used to measure ascending and descending aortic volume flow in 39 patients with aortic coarctation and in 12 healthy volunteers. Magnetic resonance imaging was also used for anatomic and peak jet velocity measurements. The latter were compared with those available from continuous wave Doppler study in 40% of the patients.

Results. Whereas ascending aortic volume flow measurement did not show significant differences between the patient and healthy control groups, volume flow curves in the descending aorta did show significant differences between the two groups. Peak volume flow (mean $\pm$ SD) was 10.6 $\pm$ 5.3 liters/min in patients and 19.6 $\pm$ 4.7 liters/min in control subjects (p < 0.001). Time-averaged flow was 2.5 $\pm$ 0.9 liters/min in patients and 3.9 $\pm$ 1.1 liters/min in control subjects (p < 0.05). The descending/ascending aorta flow ratio was 0.47 $\pm$ 0.19 in patients and 0.64 $\pm$ 0.08 in control subjects (p < 0.05). These variables correlate well with the degree of aortic narrowing. Peak coarctation jet velocity measured by MRI velocity mapping is comparable to that obtained from continuous wave Doppler study (r = 0.95).

Conclusions. We established normal ranges for volume flow in the descending aorta and demonstrated abnormalities in patients with aortic coarctation. These abnormalities are likely to be related to resistance to flow imposed by the coarctation and could represent an additional index for monitoring patients before and after intervention.

(J Am Coll Cardiol 1993;22:1515–21)

Regular follow-up of patients with aortic coarctation is important, and a noninvasive method for periodic assessment of coarctation or recoarctation is highly desirable in the preoperative and postoperative management of these patients. Techniques for evaluating aortic coarctation or recoarctation, after intervention, depend on either direct visualization of the diseased segment or study of its effect on pressure and flow.

In many centers, catheterization and angiography would normally be performed to confirm the preoperative and postoperative findings before intervention. However, the prediction of hemodynamic consequences of coarctation from an aortogram is not accurate, and volume flow cannot be measured. It also carries a risk of morbidity because it is an invasive procedure.

Imaging by two-dimensional echocardiography is unreliable because it may be difficult to obtain a good echo window (1), but continuous wave Doppler measurements are useful for predicting the presence of a gradient (2–4). However, accurate descending aorta volume flow measurement is not possible with ultrasound because of the difficulties of access and the complexity of flow.

An alternative method is magnetic resonance imaging (MRI), which can provide high resolution, dimensionally accurate images of aortic coarctation (5–8). In addition, MRI velocity mapping is the only technique able to measure volume flow reliably in the descending aorta, and it can do this by accurate measurement of multiple velocity points across the area transecting the aorta. The principles of this technique, its validation and clinical applications have been reviewed elsewhere (9).

This study is primarily concerned with the characterization of flow waveforms and the measurement of volume flow in the ascending and descending thoracic aorta of patients with aortic coarctation and of healthy volunteers. We present the method and discuss the relation between aortic narrowing and peak instantaneous and time-averaged flow

Table 1. Clinical Characteristics of Study Patients

Pt No.	Age (yr)/ Gender	Intervention	Interval (yr)	AA Flow (liters/ min)	DA Flow (liters/ min)	DA/AA Ratio	Peak AA Flow (liters/ min)	Peak DA Flow (liters/ min)	Peak Ratio DA/AA	MRV (m/s)	Diameter Coarc (mm)	Doppler (m/s)	Comment
1	18/M	Resection	12	7.2	4.2	0.58	22.9	13.5	0.59	2.4	12	2.5	
2	50/M	Resection + homograft	35	7.5	2.2	0.29	27.5	6.1	0.22	3.8	8	3.9	
3	17/M	Resection	14	7.3	0.6	0.08	33.4	3.9	0.12	3.8	9	3.2	
4	21/F	Resection	20	5.7	3.6	0.63	23.6	13.0	0.55	2.6	10	2.7	
5	32/F	Dacron patch	19	4.1	2.3	0.56	21.3	14.0	0.65	—	19	—	
6	08/M	—	—	2.9	1.6	0.55	11.1	4.8	0.43	1.6	6	—	
7	42/M	Dacron patch	25	5.0	2.6	0.52	24.8	13.8	0.56	1.6	11	—	
8	22/M	Resection	21	5.9	2.8	0.47	34.5	10.3	0.30	3.6	11	3.6	
9	17/F	Dacron patch	12	5.9	1.8	0.30	26.3	8.7	0.33	1.9	10	—	
10	21/F	—	—	5.2	2.8	0.54	19.3	7.6	0.39	2.0	5	—	Poststenotic aneurysm
11	11/M	Subclavian AF	12	4.1	2.8	0.68	20.5	13.3	0.65	2.7	11	—	
12	11/M	Subclavian AF	11	4.5	3.0	0.67	18.8	9.5	0.51	2.0	10	—	
13	13/M	PCBD	0.3	4.3	3.3	0.69	18.6	12.1	0.65	1.6	14	—	
14	28/M	Resection	24	5.0	3.2	0.64	26.3	14.8	0.56	2.1	12	—	
15	28/M	PCBD	2	6.0	4.4	0.73	24.6	13.8	0.56	1.8	11	1.7	
16	12/M	Subclavian AF	12	3.4	2.2	0.65	16.0	10.7	0.66	1.7	12	1.7	
17	18/M	Dacron conduit	16	6.7	3.4	0.51	25.7	13.4	0.52	—	16	—	Long, tortuous segment
18	28/M	Resection	23	7.4	3.3	0.45	35.2	18.2	0.51	2.0	17	—	
19	10/F	Subclavian AF	9	3.2	2.2	0.68	13.9	10.6	0.76	1.9	11	2.1	
20	20/F	PCBD	0.5	8.0	3.0	0.38	36.9	5.7	0.15	3.8	6.5	3.5	
21	14/F	IMA patch	5	4.3	2.4	0.56	21.6	7.7	0.36	1.7	8	—	
22	16/M	Resection	—	4.8	1.7	0.35	22.0	3.6	0.16	3.0	6	—	
23	25/M	Resection	21	3.9	2.5	0.64	22.4	12.9	0.58	2.8	16	—	
24	18/M	IMA patch	16	4.7	3.0	0.64	25.3	19.7	0.78	1.6	12	—	
25	20/M	Subclavian AF	13	5.0	0.8	0.16	18.8	1.9	0.10	—	2	—	Long, tortuous segment
26	26/F	Resection	21	5.7	2.5	0.44	25.2	12.0	0.48	1.8	11	—	Closure of PDA
27	36/M	Resection	30	5.8	2.5	0.43	27.1	15.1	0.58	1.8	14	—	
28	18/M	PCBD	3	3.7	2.3	0.63	15.6	9.3	0.60	2.7	9	3.3	
29	27/M	PCBD	3	7.4	2.9	0.39	31.8	10.6	0.33	2.0	11	2.1	
30	26/F	Resection	14	5.1	2.9	0.57	21.6	12.0	0.56	1.8	9.5	—	
31	35/F	Resection + Dacron patch	24	5.2	2.1	0.40	29.3	3.7	0.13	3.6	10	—	
32	32/M	Resection	18	5.6	3.6	0.64	35.1	26.3	0.75	2.0	19	2.0	Aortic regurgitation
33	10/M	Subclavian AF	10	2.8	1.3	0.46	14.3	6.0	0.42	2.0	11	2.1	
34	04/F	Subclavian AF	3	2.0	1.4	0.70	7.2	5.4	0.75	1.5	8	—	
35	03/M	PCBD	1	2.5	1.3	0.52	9.0	3.9	0.43	1.7	8	2.1	
36	55/M	—	35	6.1	3.1	0.50	36.0	21.0	0.58	2.0	14	—	
37	26/M	Resection	19	7.9	3.5	0.44	36.0	14.0	0.39	4.0	9	—	
38	10/M	PCBD	8	2.9	2.0	0.69	14.0	5.6	0.40	2.9	7	3.0	
39	11/F	PCBD	1	3.6	1.3	0.36	12.7	4.2	0.33	2.4	8	3.0	

AA = ascending aorta; AF = artery flap; Coarc = coarctation; DA = descending aorta; F = female; IMA = internal mammary artery; Interval = interval between intervention and investigation; M = male; MRV = magnetic resonance velocity mapping; PCBD = percutaneous balloon dilation; PDA = patent ductus arteriosus; Pt = patient.

measurement. Finally, we compare peak coarctation jet velocity measured by MRI velocity mapping with that obtained from continuous wave Doppler echocardiography.

Methods

Patients. Thirty-nine patients with aortic coarctation (27 male, 12 female) who were referred for evaluation of aortic anatomy by MRI were the subjects of our study (Table

1). Twelve healthy volunteers were studied for comparison (Table 2). Children <10 years old received oral sedation with chloral hydrate (30 mg/kg body weight) approximately 1 h before the investigation.

Magnetic resonance imaging. A Picker International Vista MR 2055 scanner operating at 0.5 T was used with a surface receiver coil and electrocardiographic gating. Multi-slice spin echo (echo delay time [TE] 40 ms) images were acquired in transverse, coronal, sagittal and oblique sagittal

Table 2. Clinical Features of the Control Group

Pt No.	Age (yr)/ Gender	AA Flow (liters/min)	DA Flow (liters/min)	DA/AA Ratio	Peak AA (liters/min)	Peak DA (liters/min)	Peak Ratio DA/AA
1	29/F	6.7	4.4	0.66	30.5	21.1	0.69
2	34/M	4.0	2.4	0.60	22.1	13.5	0.61
3	52/M	4.7	3.0	0.64	28.3	18.0	0.64
4	45/M	6.0	3.5	0.58	30.5	20.0	0.66
5	19/M	6.5	4.4	0.68	36.6	21.4	0.59
6	62/M	6.0	3.1	0.52	32.3	17.6	0.54
7	60/M	5.2	4.0	0.77	23.7	19.5	0.82
8	29/M	5.5	3.1	0.56	26.9	15.5	0.58
9	33/M	6.3	4.0	0.63	29.8	17.9	0.60
10	19/M	6.8	5.3	0.78	37.2	27.7	0.74
11	45/M	4.8	2.7	0.56	22.7	13.6	0.60
12	18/M	9.6	6.6	0.67	48.7	29.6	0.61
Mean	37	6.0	3.9	0.64	30.8	19.6	0.64
±SD	15	1.4	1.1	0.08	7.2	4.7	0.08

Abbreviations as in Table 1.

planes to display aortic anatomy (Fig. 1). The minimal diameter of aortic narrowing was measured and normalized for ascending aorta flow (cardiac output) because the surface area of these patients was not available to us. Slice thickness was 6 to 10 mm, and the field of view was 25 to 40 cm, with a resolution of 256 pixels in the frequency-encoding direction and 128 to 192 pixels in the phase-encoding direction. The high resolution acquisition variables were used in children. Each phase-encoding step was acquired twice and averaged so that imaging time was 3 to 4 min for each set of images, depending on heart rate. The gradient echo (TE 3.6 ms) sequence was used with and without velocity encoding to study the flow waveforms in an oblique plane perpendicular to the ascending aorta and descending thoracic aorta 5 to 10 mm distal to the coarctation, with velocity encoded through the imaging plane (slice-select direction) (Fig. 2). Instantaneous flow at 16 stages through the cardiac cycle was calculated from the cross-sectional area of the vessel and the mean velocity within this area (Fig. 2). A graph of instantaneous flow at each frame of the acquisition was then plotted against gating delay to plot a time-flow curve (Fig. 3). Mean volume flow was computed from the area under the curve.

Peak coarctation jet velocity mapping was acquired in the plane of the aortic coarctation, with velocity being encoded vertically (read direction) (Fig. 1B). Peak velocity was measured by searching the jet region for the maximal pixels. Peak velocity pixels were only accepted if a minimum of four pixels with comparable values was found. The MRI investigator was unaware of the Doppler data.

Doppler echocardiography. Peak coarctation jet velocity measured by MRI velocity mapping was compared with that measured by Doppler echocardiography in 15 of our patients (40%) who had Doppler echocardiographic measurements performed on the same day as the MRI study. The Doppler study was executed and evaluated with a Hewlett-Packard 2-MHz continuous wave Doppler echocardiograph by an experienced echocardiographer who was unaware of the MRI data. Children <10 years old received oral sedation as described earlier.

Statistical analysis. The Student t test was used to compare MRI hemodynamic data of patients with those of healthy volunteers. Linear regression analysis was used to assess the relation between MRI measurement of aortic narrowing and MRI hemodynamic data (Fig. 4 to 6). Comparison of peak coarctation jet velocity by MRI and Doppler study was analyzed using linear regression analysis and the method described by Bland and Altman (10) (Fig. 7).

Results

Magnetic resonance spin echo images acquired for anatomic display and MRI flow mapping acquired for measurement of instantaneous and time-averaged flow in the ascending and descending aorta were satisfactory in all patients (Table 1). Magnetic resonance imaging measurement of coarctation jet velocity was successful in all but two patients who had a long, tortuous coarctation segment (Patients 17 and 25, Table 1). One patient (Patient 5, Table 1) was not comfortable, and the study was aborted before measurement of coarctation jet velocity.

Time-averaged aortic flow. Although ascending aorta flow measurements and curves did not differ significantly between patients and healthy control subjects, the following variables related to flow in the descending aorta did show significant differences between the two groups: Peak volume flow was 10.6 ± 5.3 liters/min (mean ± SD) in patients and 19.6 ± 4.7 liters/min in control subjects ($p < 0.001$); time-averaged flow was 2.5 ± 0.9 liters/min in patients and 3.9 ± 1.1 liters/min in control subjects ($p < 0.05$); and descending/ascending aorta flow ratio was 0.47 ± 0.19 in patients and 0.64 ± 0.08 in control subjects ($p < 0.05$) (Tables 1 and 2, Fig. 2 and 3).
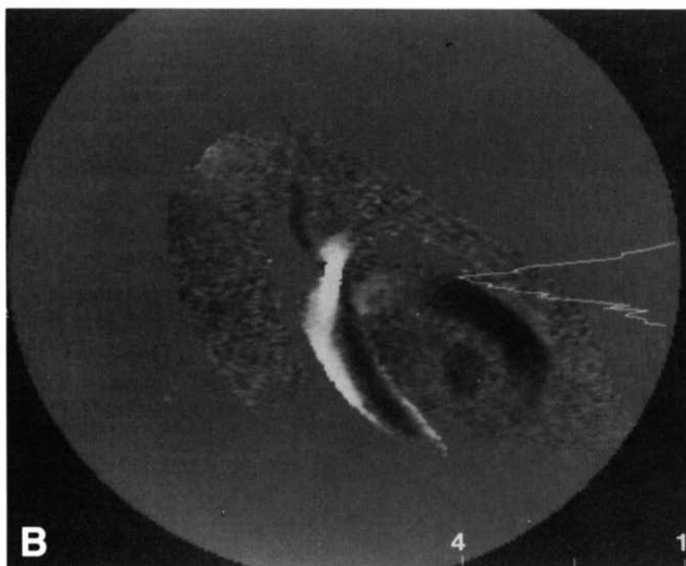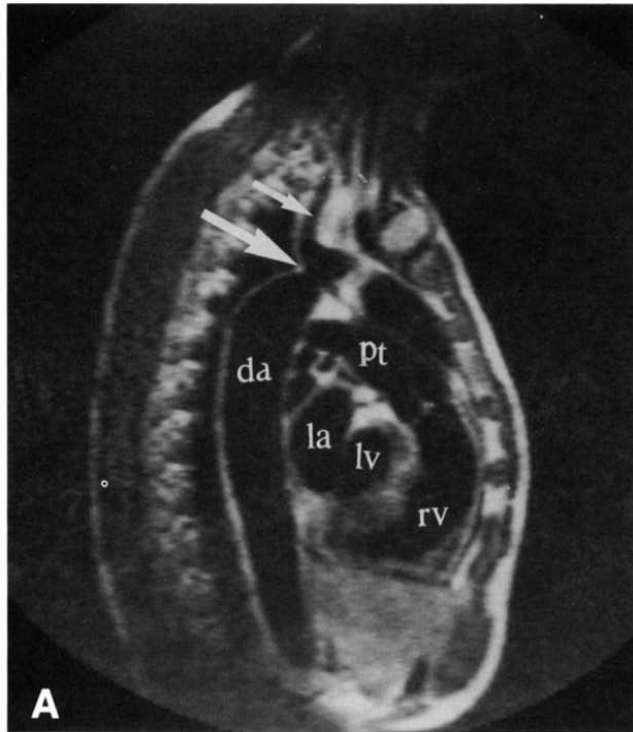
Figure 1. A, Spin echo image (echo delay time 40 ms) acquired in the sagittal plane in a patient with aortic coarctation (large arrow) and a corresponding velocity map (B) acquired during systole with a vertical velocity encoding. The sagittal plane is rotated during velocity map acquisition to align the jet with vertical read gradient direction. The velocity maps indicate zero velocity as midgray, caudal velocities in lighter shades of gray and cranial velocities in darker shades of gray. Coarctation jet velocity is seen in white, with a velocity profile (m/s) displayed in the center of the jet. A reverse flow is seen in black anterior to the jet (see Fig. 2B). Left subclavian artery (small arrow); da = descending aorta; la = left atrium; lv = left ventricle; pt = pulmonary trunk; rv = right ventricle.
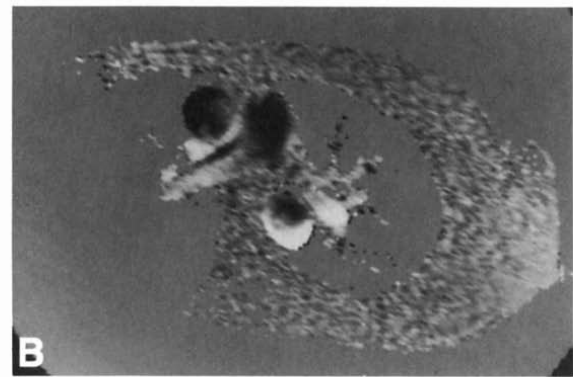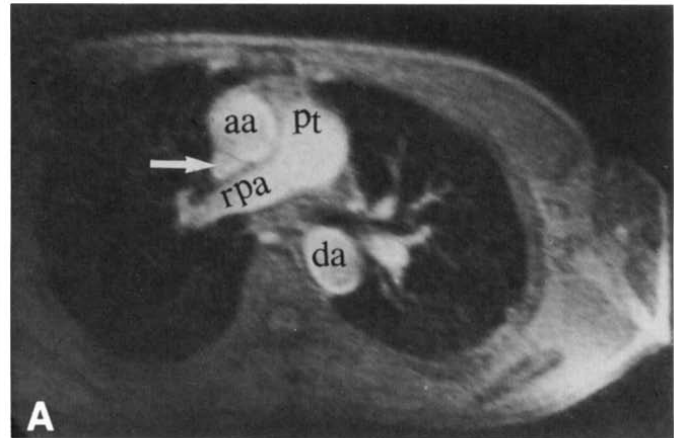
Figure 2. A, Gradient echo (echo delay time 3.6 ms) image in the plane perpendicular to the ascending and descending aorta in a patient with coarctation (shown in Fig. 1), with a velocity map (B) encoded through the plane during systole. C, Velocity map in a similar plane to that shown in A, acquired in a healthy volunteer during systole. Arrow indicates the superior vena cava. The velocity maps are shaded as in Figure 1B. aa = ascending aorta; rpa = right pulmonary artery; other abbreviations as in Figure 1.

Diameter of aortic coarctation and hemodynamic data. Aortic coarctation diameter normalized for cardiac output correlates well with descending/ascending aorta mean and peak flow ratios (r = 0.58 and r = 0.70, respectively) (Fig. 4

and 5). Peak coarctation jet velocity measured by MRI velocity mapping is inversely but poorly related to aortic diameter index (r = −0.48) (Fig. 6).

Agreement between magnetic resonance imaging velocity mapping and Doppler study. Peak coarctation jet velocity measured by MRI velocity mapping is comparable to that obtained by continuous wave Doppler echocardiography
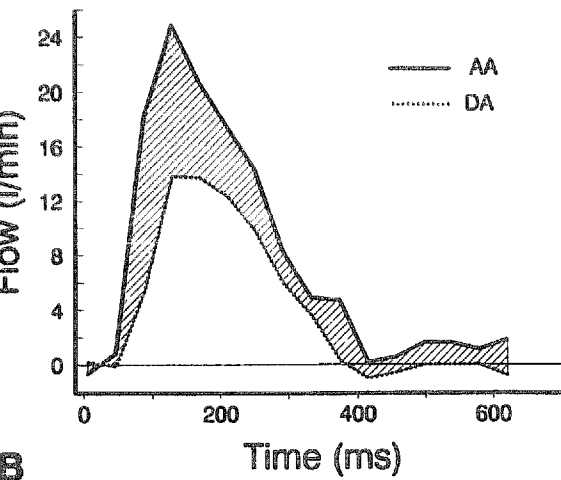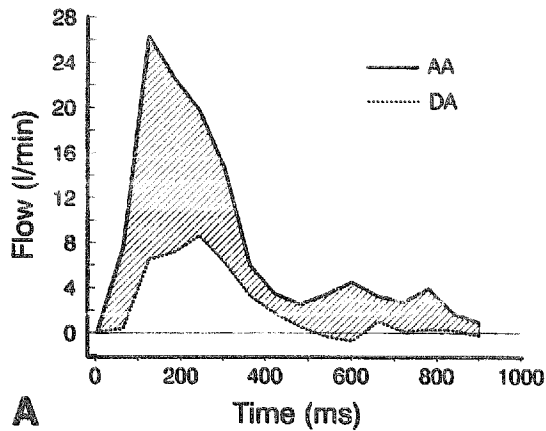
A

B

Figure 3. Flow volume curves in the ascending and descending aorta measured from the complete cine velocity map acquisition in a patient with aortic coarctation (A) and in a healthy volunteer (B). AA = ascending aorta; DA = descending aorta.

(r = 0.95) (Fig. 7A). Using the method described by Bland and Altman (10), MRI peak velocity measurements were plotted against Doppler peak velocity measurements, and

Figure 4. Mean flow ratio in the descending and ascending aorta versus aortic diameter index. y = 0.07x + 0.36. SEE = 0.102, r = 0.58. The shaded area represents the mean flow ratio in the healthy volunteers. Abbreviations as in Figure 3.
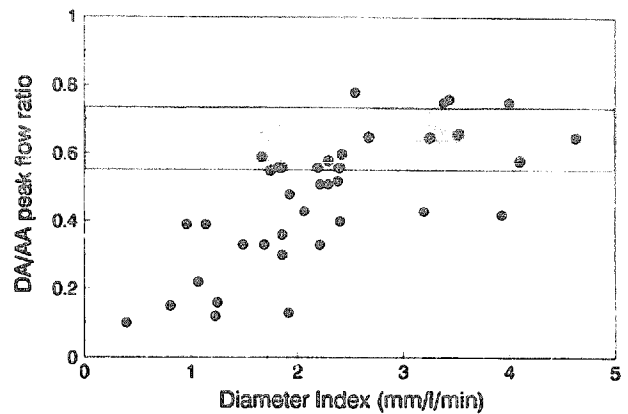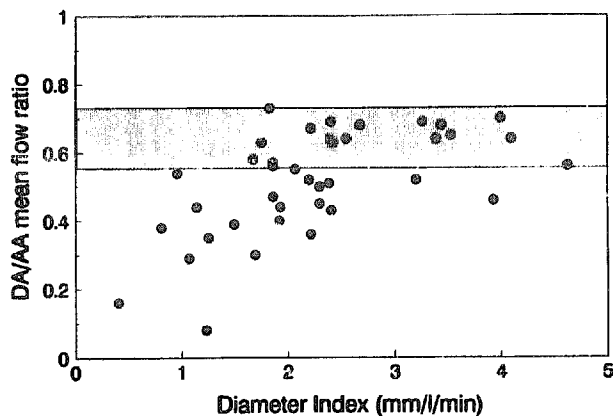

Figure 5. Peak flow ratio in the descending and ascending aorta versus aortic diameter index. y = 0.12x + 0.21, SEE = 0.120, r = 0.70. The shaded area represents the peak flow ratio in the healthy volunteers. Abbreviations as in Figure 3.

the differences were then plotted against the mean values of each pair of measurements (Fig. 7B).

Discussion

Technical considerations. Although MRI velocity mapping has been shown to be a robust technique for measurement of blood flow, until recently, marked systolic signal loss in the aorta has jeopardized measurement of blood flow and blood flow velocity in and around the coarctation segment by the gradient echo sequence with a relatively long echo time (8,11). The factor responsible for this phenomenon is mainly turbulence in which there are random velocities in space and time (12). An important advance has been the reduction in echo time (i.e., the time from the peak of the initial energizing signal to the peak of the final echo) to 3.6 ms (13). This is because at sites of stenosis, where high blood flow velocity is found, turbulence and high orders of motion cause signal loss, preventing accurate velocity mapping in this area. Shortening the echo time reduces the

Figure 6. Peak coarctation jet velocity measured by magnetic resonance velocity mapping versus aortic diameter index. y = -0.50x + 3.5, SEE = 0.757, r = -0.48.
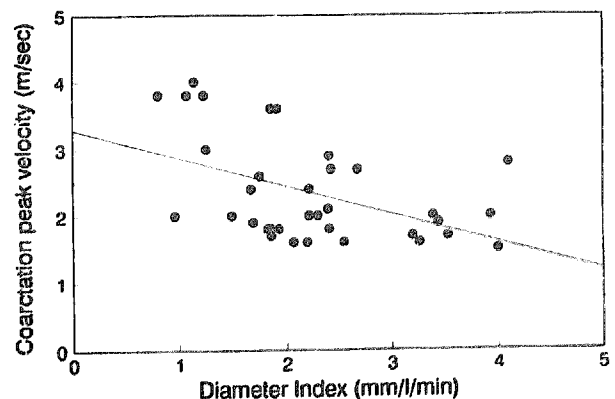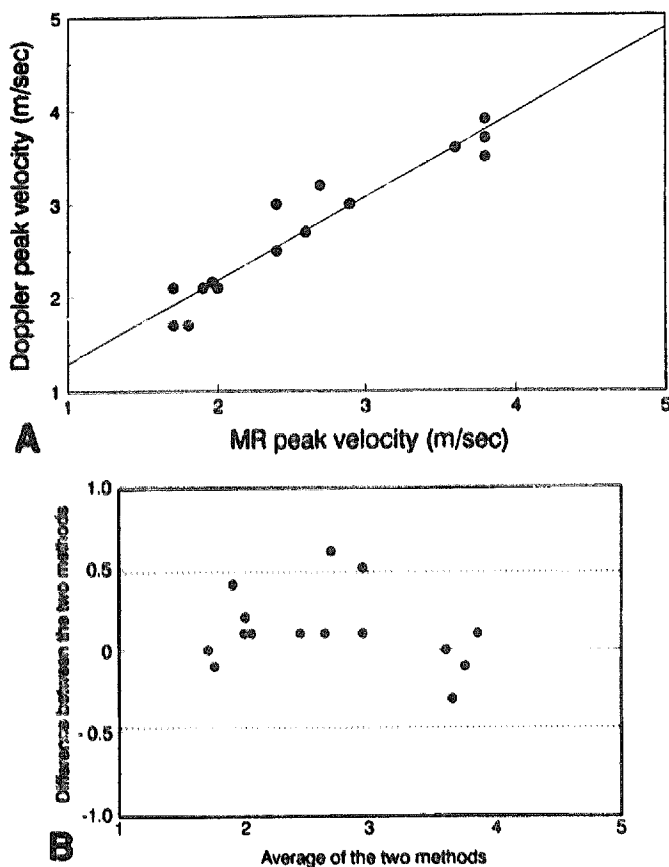
Figure 7. A, Peak coarctation jet velocity measurements by magnetic resonance imaging (NMR) plotted against those by Doppler ultrasound. y = 0.62x + 1.10. SEE = 0.151, r = 0.95. B, Difference between magnetic resonance imaging and Doppler peak velocity measurements plotted against the mean value of each pair. Mean difference 0.12; standard deviation of the difference 0.23; confidence interval (dashed lines) ±0.47, level of agreement 83%. See text for details.

period during which accelerating or turbulent flows bring about phase incoherence and loss of the final echo. The shorter the echo time, the higher the threshold of turbulence intensity at which signal is lost (14). This is also dependent on the magnetic field strength and acquisition variables (15).

Comparison between aortic flow in patients and healthy volunteers. Blood flow in the ascending and descending aorta is phasic. Although the average flow in the ascending and descending thoracic aorta in the control group is 6.0 and 3.9 liters/min, respectively, peak systolic flow in these vessels can be >40 and >30 liters/min, respectively (Fig. 3B, Table 2). In patients with aortic coarctation, flow in the ascending aorta is quantitatively and qualitatively similar to that of control subjects. However, the volume flow and the flow waveforms in the descending aorta in patients with significant coarctation are different from those in control subjects. The waveforms are markedly damped by propagation through the narrowed aortic segment, and the volume flow in this vessel is significantly reduced (Fig. 3A, Table 1).

Coarctation peak jet velocity and the modified Bernoulli equation. A common method of assessing the hemodynamic significance of coarctation is to use the modified Bernoulli equation ($\Delta P = 4V^2$, where ΔP = pressure difference [in mm Hg], and V = peak velocity [m/s]) to calculate the pressure difference across the diseased segment from the coarctation peak jet velocity measured by Doppler echocardiography (2) or by MRI velocity mapping (14). Although useful in assessing valvular disease, this approach in aortic coarctation could have potential technical and physiologic problems that could lead to underestimation of aortic narrowing. The technical problem is encountered when there is a long, tortuous coarctated segment, making it difficult to contain the coarctation jet within the image plane, therefore resulting in underestimation of velocity and the degree of aortic narrowing (Table 1). Movement of patients during or between data acquisition can lead to a similar inaccuracy. The physiologic problem is related to the state of the collateral vessels around the coarctation that lead to diversion of blood flow away from the coarctation segment to the lower part of the body. Because this will reduce the preload on the coarctation; changes in blood velocity will not reflect the true degree of aortic narrowing. This might explain the poor correlation between peak coarctation jet velocity and coarctation diameter index (Fig. 6), although inaccuracy in the measurement of aortic diameter might be another factor. It is therefore useful to measure the flow rate in addition to peak velocity measurement when assessing aortic coarctation.

Measurement of aortic flow in patients with coarctation. An alternative or complementary approach is to measure instantaneous as well as time-averaged flow distal to the aortic narrowing. This has several advantages. 1) It allows easy measurement when the coarctation segment is narrowed and tortuous, especially in small patients (Table 1, Patients 17 and 25). 2) It allows quantitative measurement of the distribution of volume flow to be performed proximal and distal to aortic narrowing, which is an important factor in the development of signs and symptoms related to aortic coarctation. It is also tempting to assume that the size of the global collateral circulation can be estimated from the differential distribution of flow in the ascending and descending thoracic aorta. 3) Characterization of the flow waveforms and measurement of peak instantaneous flow distal to the coarctation are an additional advantage. In this study we showed a relation between these measurements and aortic diameter (Fig. 4 and 5). As expected, the relation between descending/ascending aorta mean flow and aortic diameter index is curvilinear. In patients with a diameter index <3 mm/liter per min these variables show a linear relation because of the diversion of flow through the collateral vessels, whereas in patients with a diameter index >3 mm/liter per min they are within the normal range and bear no relation.

However, a potential source of error in the measurement of volume flow in the descending aorta is possible if flow measurement is acquired above or below possible collateral flow entry. A possible refinement of this technique would be

to acquire flow data, in the four dimensions of space-time, in the whole coarctation region. This should enable calculations of the volume of flow approaching an orifice to be correlated with peak jet velocity, allowing calculation of orifice area. It should also allow analysis of jet shape and downstream flow. Such analysis could have a bearing on the applicability (or otherwise) of the modified Bernoulli equation and might lead to development of new formulas for calculating the rate of energy dissipation for a given rate of flow through a particular stenosis, all of which could be relevant to decision making with regard to the timing and type of intervention.

Magnetic resonance imaging velocity mapping compared with Doppler echocardiography. Although this comparison was done in a limited number of patients, the agreement between measurements of coarctation peak jet velocity by MRI velocity mapping and Doppler ultrasonography confirms our previous reports (14-18) and indicates that the new technique has sufficient accuracy to be of clinical value. The two techniques are complementary. Magnetic resonance imaging velocity mapping is useful if the echo window is limited or alignment of the ultrasound beam is inadequate, because there is no limitation on velocity mapping for site or direction of acquisition of data. This feature has proved to be particularly valuable in patients with congenital heart disease, such as conduit stenosis (18). The other major advantage of velocity mapping is that volume flow can be calculated with high accuracy because of the simultaneous acquisition of mean velocity and area of the vessel. Doppler echocardiography is accurate for measuring velocity but poor at assessing volume flow, especially when the flow pattern is complex (Fig. 1 and 2).

Limitations of magnetic resonance imaging velocity mapping. The limitations of cine MRI velocity mapping include the relatively long acquisition times, the poor quality of cardiac gated images in patients who have cardiac arrhythmias, the confined bore of the magnet (which may preclude use of the technique in patients with claustrophobia) and the high cost of the machine. These limitations may become less important with the development of real-time MRI velocity mapping using an echo planar or other rapid imaging techniques (19-21), open access magnets and cheaper hardware.

Conclusions. Magnetic resonance imaging can provide noninvasive measurements of changes in aortic flow. We established normal ranges and demonstrated abnormalities in patients with aortic coarctation. These abnormalities are most likely related to resistance to flow imposed by the coarctation segment and could represent an additional index for monitoring the hemodynamic significance of coarctation or recoarctation in patients before and after intervention.

References

1. Sahn DJ, Allen HD, McDonald G, Goldberg SJ. Real-time cross sectional echocardiographic diagnosis of coarctation of the aorta. Circulation 1977;56:762-91.
2. Wyse RKH, Robinson PJ, Deanfield JE, Tunstall Pedoe DS, Macartney FJ. Use of continuous wave Doppler ultrasound to assess the severity of coarctation of the aorta by measurement of aortic flow velocities. Br Heart J 1984;52:278-83.
3. Marx GR, Allen HD. Accuracy and pitfalls of Doppler evaluation of the pressure gradient in aortic coarctation. J Am Coll Cardiol 1986;7:1379-85.
4. Hoadley SD, Duster MC, Miller JF, Murgo JP. Pulsed Doppler study of a case of coarctation of the aorta: demonstration of a continuous Doppler frequency shift. Pediatr Cardiol 1986;6:275-7.
5. Amparo EG, Higgins CB, Shafton EP. Demonstration of coarctation of the aorta by magnetic resonance imaging. Am J Roentgenol 1984;143:1192-4.
6. von Schulthess GK, Higashino SM, Higgins SS, Didier D, Fisher MR, Higgins CB. Coarctation of the aorta: MR imaging. Radiology 1986;158:469-75.
7. Boxer RA, LaCorte MA, Singh S, et al. Nuclear magnetic resonance imaging in evaluation and follow-up of children treated for coarctation of the aorta. J Am Coll Cardiol 1986;7:1095-8.
8. Rees RSO, Somerville J, Ward C, et al. Magnetic resonance imaging in late post-operative assessment of coarctation of the aorta. Radiology 1989;173:499-502.
9. Mohiaddin RH, Longmore DB. Functional aspects of cardiovascular nuclear magnetic resonance imaging. Techniques and application. Circulation 1993;88:264-81.
10. Bland JM, Altman DG. Statistical methods for assessing agreement between two methods of clinical measurement. Lancet 1986;1:307-10.
11. Simpson IA, Chung KJ, Glass RF, Sahn DJ, Sherman FS, Hesselink J. Cine magnetic resonance imaging for evaluation of anatomy and flow relations in infants and children with coarctation of the aorta. Circulation 1988;78:142-8.
12. Utz JA, Herfkens RJ, Heinsimer JA, Shimakawa A, Glover G, Pelc N. Valvular regurgitation: dynamic MR imaging. Radiology 1988;168:91-4.
13. Firmin DN, Nayler GL, Kilner PJ, Longmore DB. The application of phase shifts in NMR for flow measurement. Magn Reson Med 1990;14:230-41.
14. Kilner PJ, Firmin DN, Rees RSO, et al. Valve and great vessel stenosis: assessment with MR jet velocity mapping. Radiology 1991;178:229-35.
15. Mostbeck GH, Caputo GR, Madjumdar S, Dulce M, Shimakawa A, Higgins CB. Assessment of vascular stenoses with MR jet phase velocity mapping at 1.5T: in vitro validation [abstract]. Soc Magn Reson Med 1991;10:1272.
16. Mohiaddin RH, Amanuma M, Kilner PJ, Pennell DJ, Manzara CC, Longmore DB. Magnetic resonance phase-shift velocity mapping of mitral and pulmonary venous flow. J Comput Assist Tomogr 1991;15:237-43.
17. Kilner PJ, Manzara CC, Mohiaddin RH, et al. Magnetic resonance jet velocity mapping in mitral and aortic valve stenosis. Circulation 1993;87:1239-48.
18. Martinez JE, Mohiaddin RH, Kilner PJ, et al. Obstruction in extracardiac ventriculopulmonary conduits: value of magnetic resonance imaging with velocity mapping and Doppler echocardiography. J Am Coll Cardiol 1992;20:338-44.
19. Firmin DN, Klipstein RH, Hounsfield GL, Paley MP, Longmore DB. Echo-planar flow velocity mapping in high resolution. Magn Reson Med 1989;12:316-27.
20. Firmin DN, Gatehouse PD, Longmore DB. Comparison of snap-shot quantitative flow imaging techniques [abstract]. Soc Magn Reson Med 1992;11:2915.
21. Gatehouse PD, Firmin DN, Hughes RL, Collins S, Longmore DB. Phase contrast velocity mapping by spiral scanning [abstract]. Soc Magn Reson Med 1992;11:216.